2026 JULY 19–22 VANCOUVER, BC
JOINT AAPM | COMP MEETING

AI-Driven Radiacoustic Imaging for Proton Therapy Monitoring

Prabodh Kumar Pandey[1], Leshan Sun[1], Lucia Rodriguez Gonzalez[1], Kristina Bjegovic[1], Yuchen Song[2], Prishita Mirchandani Budhrani[2], Marti Roper[2], Yong Chen[2] and **Liangzhong Xiang**[1] (email: liangzhx@hs.uci.edu).

(1) University of California, Irvine, Irvine, CA (2)University of Oklahoma Health Sciences Center, Oklahoma City, OK

TRUE Lab

Introduction

- No clinical imaging modality can directly visualize radiation therapy (RT) in real time during treatment.
- We present radiacoustic imaging (RAI)[1], a clinically integrated platform for noninvasive, real-time, three-dimensional imaging of proton energy deposition in deep tissue using a 256-element matrix ultrasound array, synchronized parallel acquisition, and AI-based reconstruction to achieve accurate, high-frame-rate volumetric imaging.
- RAI detects acoustic waves generated by radiation-induced thermoelastic expansion[2]. Because the radiacoustic (RA) signals originate at the site of dose deposition, they encode the delivered radiation field.
- RA signals enable 3D dose map reconstruction using image reconstruction algorithms[3,4].

Here we focus on AI-driven frameworks for (A) RA signal denoising, and (B) RAI dose map reconstruction.

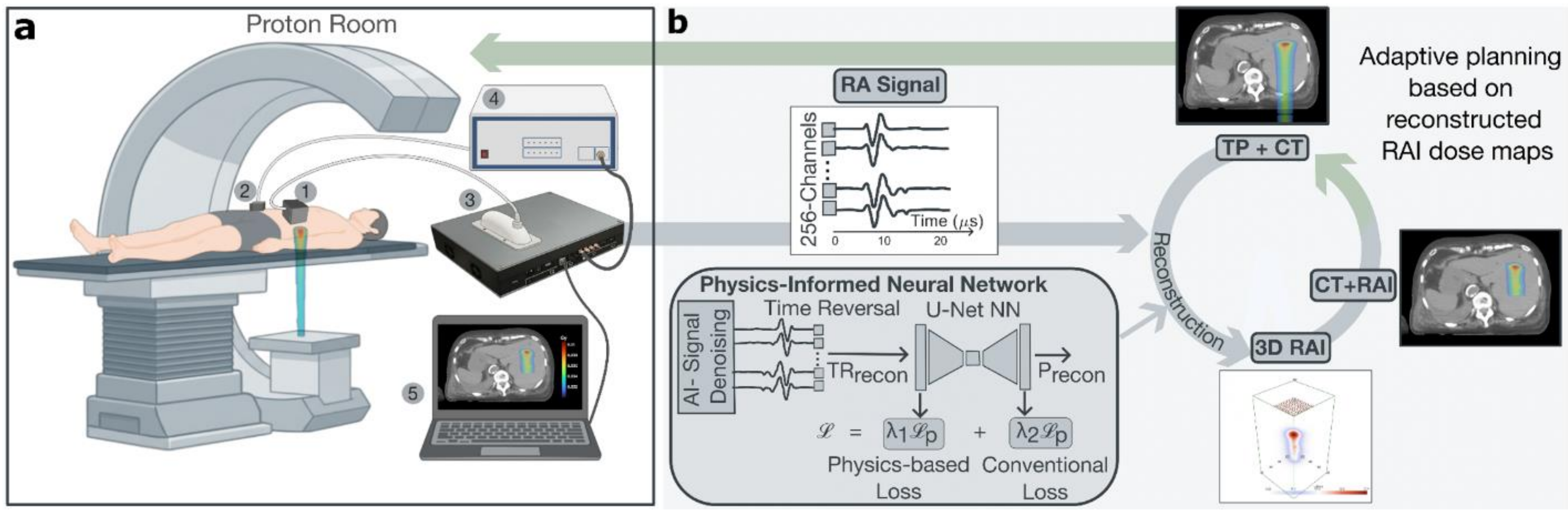

Fig. 1 | **a**, Schematic of the radiacoustic imaging (RAI) platform. **b**, AI-driven reconstruction workflow integrating AI-based denoising and image reconstruction frameworks to generate volumetric maps of proton energy deposition co-registered with CT anatomy.

AI-driven Signal Denoising

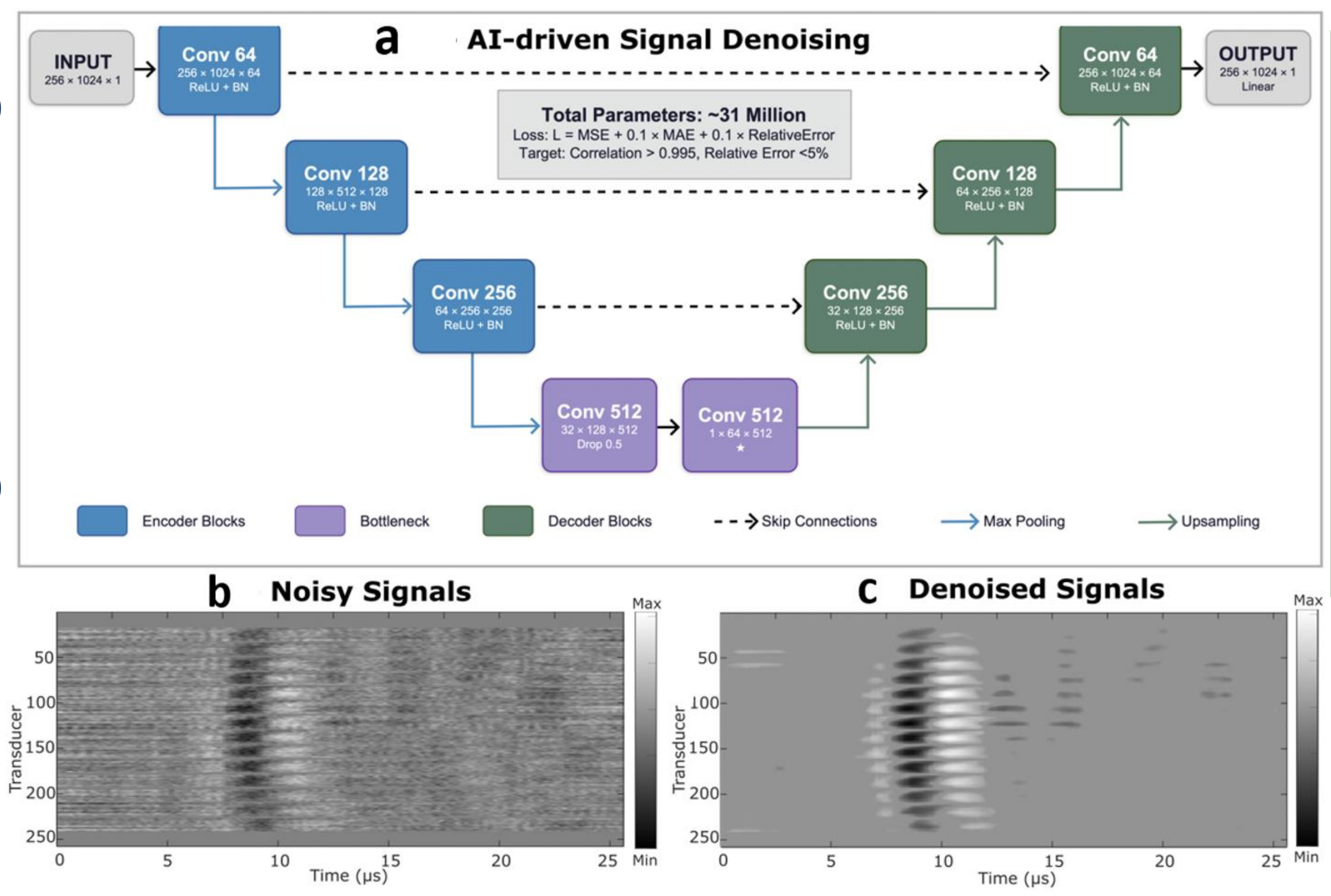

- Raw RA signals carry EM interference[5].
- A 2D U-Net learns the mapping from 10-frame inputs to >100-frame ground truth sinograms.
- The model produces denoised RA signals

Fig. 2. a, Architecture of the 2D U-Net for RF signal denoising. **b,** Representative sinogram and **c,** corresponding denoised sinogram,

AI-driven Image Reconstruction

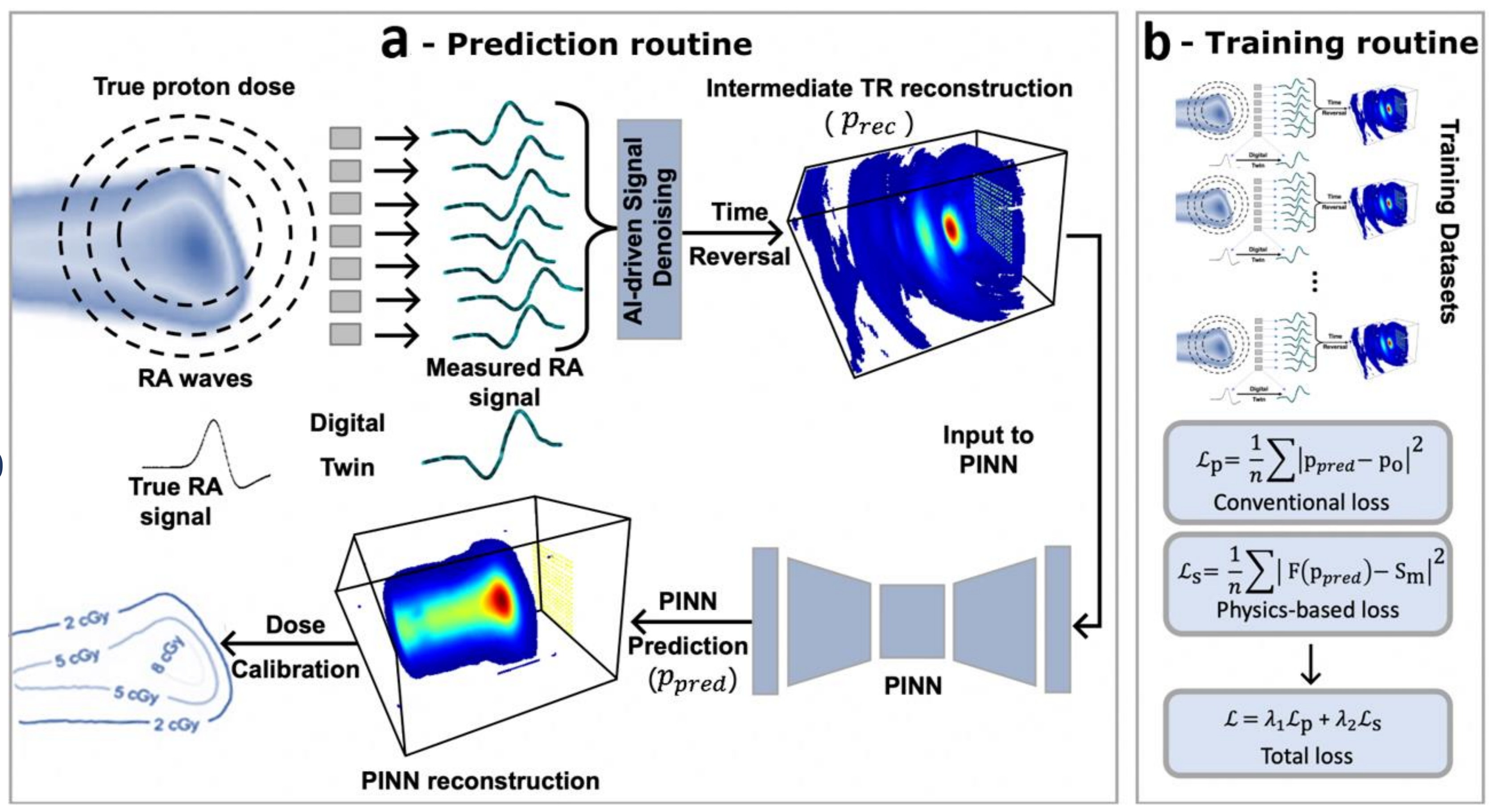

- Denoised signals are time-reversed to obtain pressure map p_{rec} with limited-view artifacts.
- p_{rec} is refined using a physics-informed AI model to an enhanced map p_{pred}, converted to quantitative dose map
- Training minimizes a combined loss composed of an image-domain term $\mathcal{L}_p$ and a sinogram-domain term $\mathcal{L}_s$[4].

Fig. 3. a, Physics-informed prediction pipeline. **b,** Training framework.

Results & Discussion

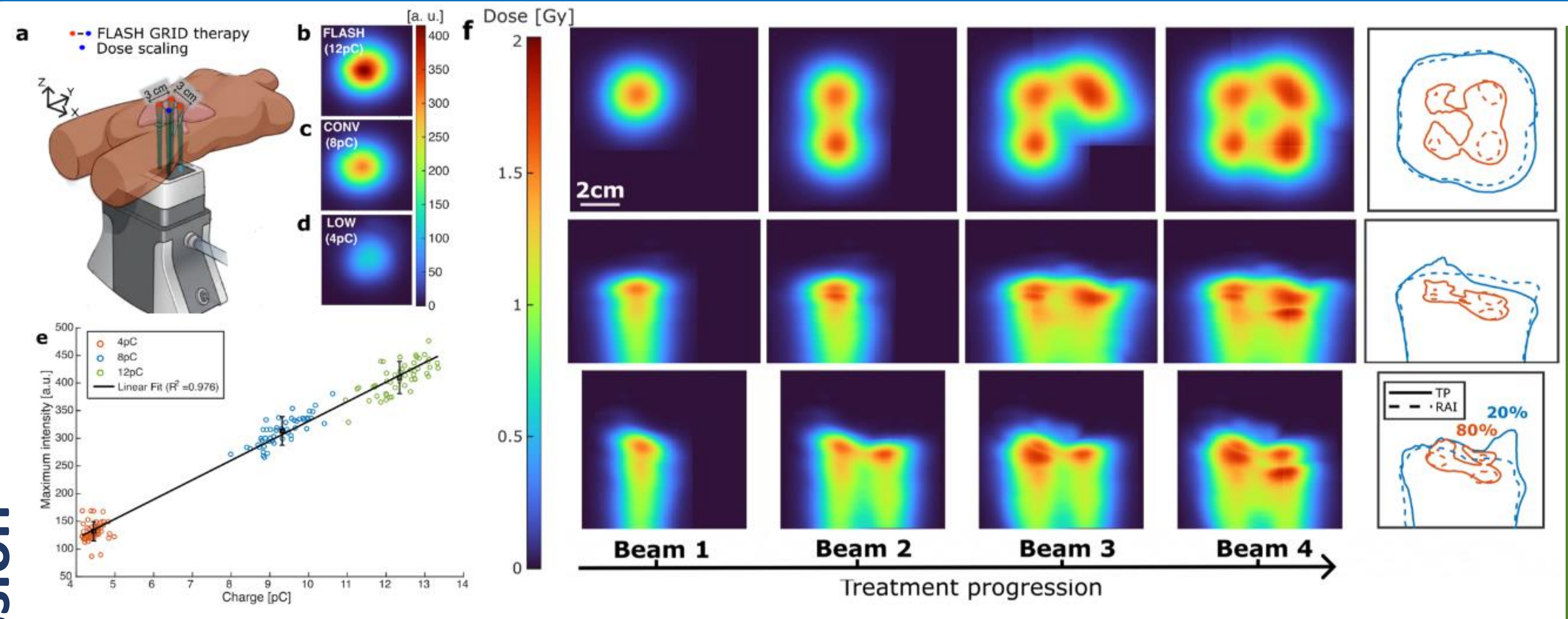

Fig. 4. Real-time volumetric imaging of proton energy deposition during FLASH-GRID irradiation. a, Schematic for RAI in a human-sized torso phantom, **b-d,** RAI MIPs at increasing charge per pulse and **e,** its linear relationship with delivered charge (R² ≈ 0.98). **f,** Time-resolved MIPs of RAI reconstructions showing progressive 3D dose accumulation and preservation of the GRID peak–valley pattern; final 20% and 80% isodose contours agree with treatment planning.

- RAI achieved localization bias below 0.3 mm at depths of 3–9 cm.
- RA signal and reconstructed RAI map scaled linearly with delivered charge across 4–12 pC/pulse with $R^2 \approx 0.98$ and without saturation.
- FLASH-GRID phantom delivery reproduced the peak–valley dose structure with 88.65% gamma pass rate (5 mm/5%).
- Volumetric imaging achievable at up to 375 Hz frame rate.
- In vivo rabbit studies yielded gamma pass rates of 94.80–94.99% (5 mm/5%).
- Clinical pencil-beam scanning liver treatment in a human cadaver achieved a 99.35% gamma pass rate (5 mm/5%).
- Skull correction for transcranial RAI reduced Bragg peak mislocalization by ~5 mm and improved gamma pass rate from 57.03% to 59.82%.

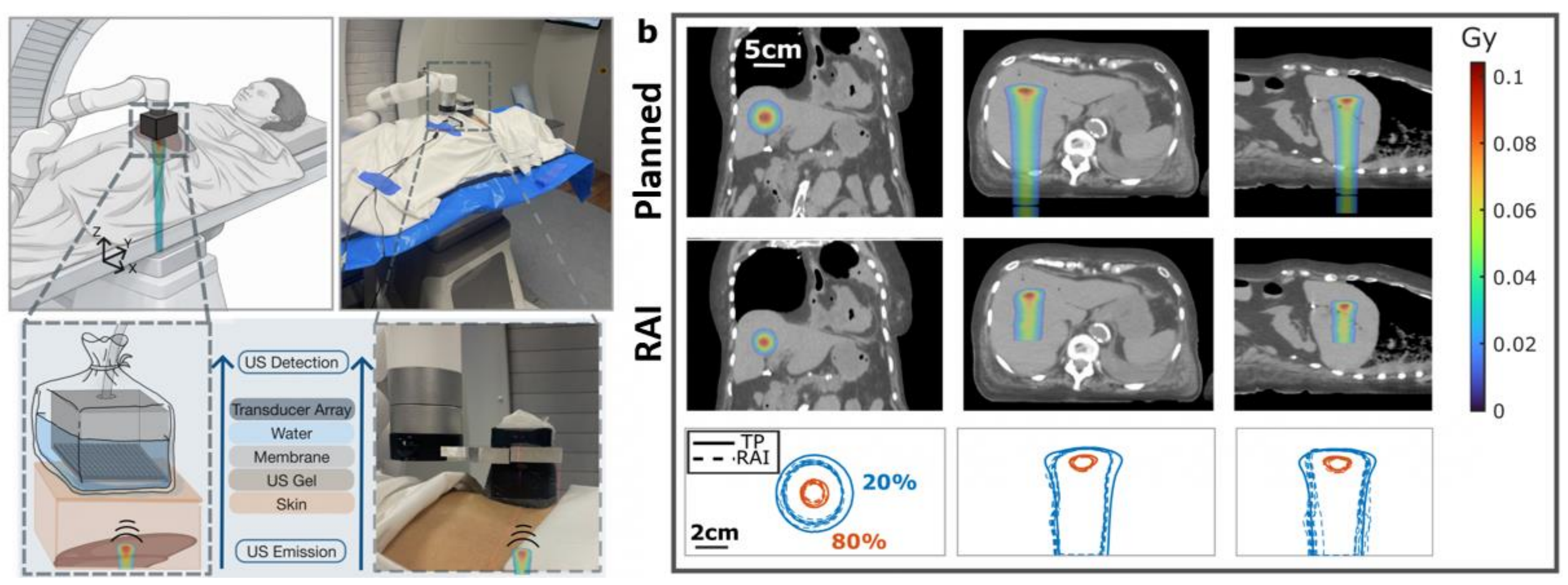

Fig. 5. RAI of proton energy deposition in the human liver. a, Schematic, clinical setup and robotic positioning of the ultrasound array for RAI acquisition from proton RT of human liver . **b,** CT-overlaid treatment planning and reconstructed RAI maps, and 20% and 80% isodose contours comparing treatment planning and RAI.

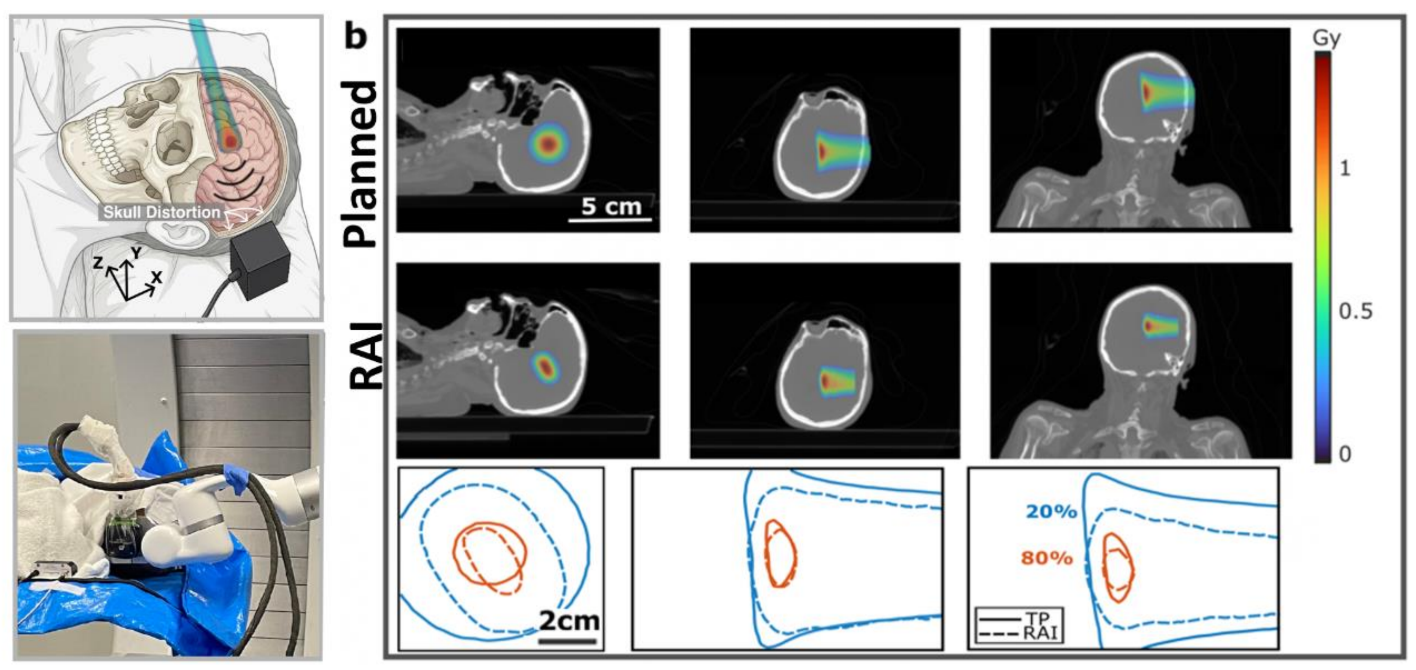

Fig. 6. Transcranial RAI of proton energy deposition in the human brain. a, Schematic, clinical setup for transcranial RAI acquisition. **b,** CT-overlaid treatment planning and skull-corrected RAI maps, and 20% and 80% isodose contours comparing treatment planning and corrected RAI.

Conclusions

- Fully AI-driven real-time 3D reconstruction of proton energy deposition in deep human tissue.
- Capable of submillimeter localization and accurate volumetric dose mapping at high frame rate.
- Heterogeneous acoustic correction enables transcranial dose imaging through the human skull.
- Future models will aim at single-pulse inference and improved correction for acoustic heterogeneities.
- AI-integrated RAI establishes the algorithmic foundation for adaptive, closed-loop RT.

Acknowledgement & COI

This work was supported by the National Institutes of Health (Nos. R37CA240806, U01CA288351, and R50CA283816). The authors would like to acknowledge the support from the UCI Chao Family Comprehensive Cancer Center (No. P30CA062203).

Liangzhong Xiang has financial interest in SoundDose, Inc., which, however did not support this work. Remaining authors have no COI.

References

1. Xu, Yifei, and Shawn Liangzhong Xiang. "Radiacoustic imaging." Nature Reviews Physics 7.11 (2025): 660-670.
2. Caron, Joseph, et al. "Single pulse protoacoustic range verification using a clinical synchrocyclotron." Physics in Medicine & Biology 68.4 (2023): 045011.
3. Pandey, Prabodh Kumar, et al. "Model-based X-ray-induced acoustic computed tomography." IEEE transactions on ultrasonics, ferroelectrics, and frequency control 68.12 (2021): 3560-3569.
4. Sun, Leshan, et al. "A Physics-Informed Neural Network For In Vivo Dosimetry Using Quantitative Radiacoustic Imaging." (2026).
5. Wang, Siqi, et al. "Real-time tracking of the Bragg peak during proton therapy via 3D protoacoustic Imaging in a clinical scenario." npj Imaging 2.1 (2024): 34.